Indian Journal of Pure & Applied Physics
Vol. 53, August 2015, pp. 537-545

Novel first-order all-pass filter applications of z-copy voltage differencing current conveyor

Roman Sotner[1], Norbert Herencsar[2], Jan Jerabek[2], Kamil Vrba[2], Tomas Dostal[1], Winai Jaikla[3]* & Bilgin Metin[4]

[1]Department of Radio Electronics, Brno University of Technology, Technicka 3082/12, 616 00 Brno, Czech Republic

[2]Department of Telecommunications, Brno University of Technology, Technicka 3082/12, 616 00 Brno, Czech Republic

[3]Department of Engineering Education, Faculty of Industrial Education, King Mongkut's Institute of Technology Ladkrabag, Ladkrabag, Bangkok 105 20, Thailand

[4]Department of Management Information Systems, Bogazici University, Hisar Campus, 34342-Bebek-Istanbul, Turkey

*E-mail: winai.ja@hotmail.com, bilgin.metin@boun.edu.tr

Received 18 April 2014; revised 27 November 2014; accepted 18 February 2015

The application of z-copy voltage differencing current conveyor (ZC-VDCC) in simple and interesting first-order all-pass sections has been studied in the present paper. The solutions presented here have presumptions for direct electronic control. Some of proposed circuits offer curious possibilities of control. Electronic controllability of the VDCC allows simultaneous zero and pole frequency adjusting, separated zero or pole frequency adjusting or migration of zero from left half plane to right half plane of complex space. Behavioral models of VDCC based on commercially available devices are proposed and selected type of all-pass section was verified by simulations and also by measurements. Results of simulations, experiments, and theoretical proposal are compared. Experiments confirm workability of proposed behavioral equivalent circuit in bandwidths to units of MHz.

Keywords: All-pass section, Behavioral modeling, Electronic control, Voltage differencing current conveyor, Z-copy, VDCC, Zero/pole location control

1 Introduction

Simple and tunable or partially adjustable active filters in both current- or voltage-mode are very useful for applications in communication subsystems like anti-aliasing or reconstruction filters and smoothers, band selection, signal generation in sine wave oscillators (all-pass or band-pass sections), etc. Simple all-pass sections are core elements of multiphase generating solutions[1-3]. Moreover, they can be used as sub-blocks for construction of the fractional order synthesis[4-7] as an example. When cascaded or interconnected, sub-blocks with adjustable location of zeros or poles can be used for approximation of fractional order "passive" elements and two-ports[4,7] or whole applications[5,6,8].

Active element used as the main core of proposed applications, is known as voltage differencing current conveyor (VDCC) and belongs to family of hybrid elements introduced by Biolek *et al*[9]. The VDCC is presented as z-copy (ZC-VDCC) variant[9] in this contribution. Several solutions of active element based on current conveyor of second generation[9-13] (CCII) and transconductance section[9,14] (OTA) were theoretically proposed. Some basic elements offer benefits of simple electronic control of intrinsic resistance (R_x) of current input terminal[11] X or current gain between X and Z terminals[12,13] by bias current. The basic building parts have been already used for construction of combined active elements with many benefits. For example, current conveyor transconductance amplifier[9,15] (CCTA) utilizes same types of sub-blocks (CCII and OTA) as VDCC, but in different order of interconnection. However, basic CCTA does not provide differential voltage input and internal transfers between main and auxiliary terminals that are important for applications.

Many all-pass structures were proposed in recent years. However, some of them are too complicated (many active and passive elements) and focused on second-order types[16,17] for example or are not supposed for direct electronic control of their parameters (neither zero/pole frequency adjusting). Of course, all-pass response is also available in second-order multi-functional biquad systems[18], but independent control of pole/zero frequency in such systems is too complex. Really simple first-order all-

pass circuits exist in the literature[19] electronic controllability is still challenging question in the hitherto literature.

The difference between VDCC and DVCC inheres from basic behaviour. The DVCC realizes subtraction of two voltages[16-19] (two differential voltage input terminals Y) and the rest of ideal behaviour is identical to classical current conveyor[9] with one current input terminal X and current output terminal Z (or multiple terminals ±Z). In comparison to DVCC, the VDCC element contains transconductance section[9] and offers additional terminal, which increases the universality of this element. Advanced CCTA with differential difference[18] CCTA (DDCCTA) has similar input features as DDCC (three Y terminals). However, ZC-VDCC proposed in this paper is more suitable for our purpose (differential input section is sufficient in many cases).

Our work is focused mainly on discussion of simple first-order all-pass sections. Therefore, a short comparison of previously published works in this field (all-pass structures based on devices similar to proposed VDCC) is necessary at this place.

Let us compare circuits based on DVCC with similar complexity: Minaei *et al*[20]. proposed general admittance networks employing one DVCC leading to specific selection of non-controllable all-pass filters, where three passive elements were required. Two DVCCs with two Y terminals (Y_1, Y_2) and one grounded capacitor were utilized in controllable (by intrinsic resistance R_x) all-pass section presented by Maheshwari *et al*[21]. The all-pass filter with the same number of active elements with one floating resistor and grounded capacitor was introduced by Minaei *et al*[22]. Horng *et al*[23]. proposed all-pass filter only with grounded passive elements, where again two DVCCs were necessary. DVCCs are useful for synthesis of the universal second-order systems, where all-pass responses are available. Interesting current-mode example has been presented by Ibrahim *et al*[24]., where three these DVCCs elements together with four grounded resistors and two grounded capacitors were used to realize all transfer characteristics.

Similar constructions of simple first-order all-pass sections are available by using of differential difference current conveyor[9] (DDCC), where not only subtraction but also addition (three or more Y terminals) is allowed. Ibrahim *et al*[25]. used one DDCC which utilizes three Y terminals, floating capacitor, and grounded resistor to realize inverting non-adjustable all-pass section. Some other solutions utilize one or two DDCCs. Combination of one floating or grounded resistor and capacitor have been introduced by Metin *et al*[26]. Solutions presented by Krishna *et al*[27]. require two DDCCs, grounded resistor and capacitor. Chatuverdi *et al*[28]. presented two DDCCs-based solutions using grounded capacitors in inverting all-pass section controllable by intrinsic resistance R_x. DDCC found its utilization also in universal second-order filtering structures. For example Ibrahim *et al*[29]. utilized dual-output DDCCs in classical KHN voltage-mode biquad solution that allows also all-pass response.

Our contribution presents several interesting current-, voltage-, and mixed-mode solutions of simple first-order all-pass transfer section employing VDCC element. Some of circuits have special electronically adjustable possibilities, e.g. zero (ω_z, f_z) or pole (ω_p, f_p) frequency control or interesting feature of their separated control. All studied circuits require minimum number of external components (only capacitors in most cases). Our solutions are simple, only differential voltage input (two voltage input terminals) is sufficient in comparison to the most similar DVCC and DDCC based solutions, where three voltage input terminals are often utilized. In addition, simple DVCC and DDCC do not have possibility of electronic control and therefore, do not provide special adjustable features.

2 Z-copy Voltage Differencing Current Conveyor

The principle of the ZC-VDCC is shown in Fig. 1, where symbol, behavioural model, and possible implementation by commercially available devices is shown. The first part of ZC-VDCC consists of OTA section with two current outputs (identical or inverted polarities) and the second part is formed by CCII section (it is current-controlled variant CCCII[11]). The active element has two voltage inputs *p*, *n*, one current input *x*, auxiliary (high-impedance) terminal *z_TA*, its copy *zc_TA* and two current outputs *zp* and *zn*. The bi-directional arrows mean both possible polarities (generally) of currents (from terminals *z_TA* and *zc_TA*).

3 Proposed Simple Filtering Applications

3.1 Current-Mode All-pass Sections

In recent years, these circuits received attention mainly as parts of multiphase oscillators[1-3]. The first example of using ZC-VDCC is shown in Fig. 2. It is

simple current-mode all-pass section with independently electronically pole frequency and also zero frequency. Transfer function of proposed circuit has form:

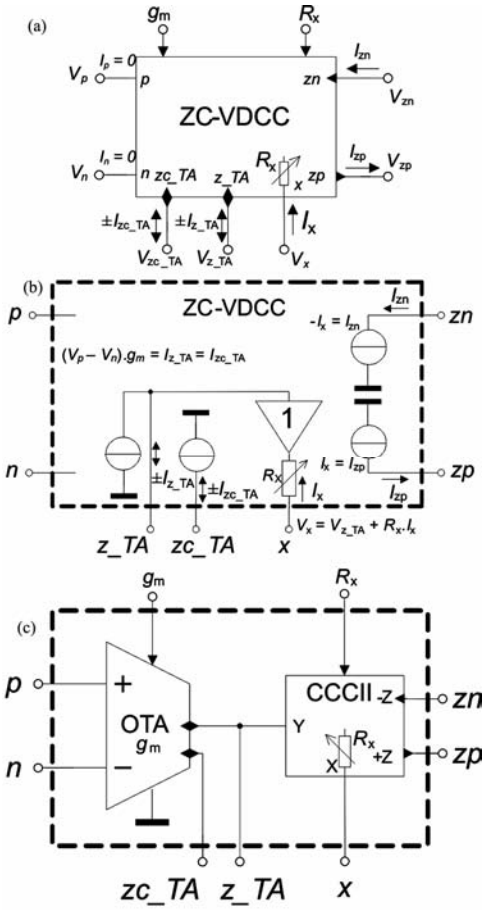

Fig. 1 — Z-copy voltage differencing current conveyor (VDCC): (a) symbol, (b) behavioral model, (c) block implementation

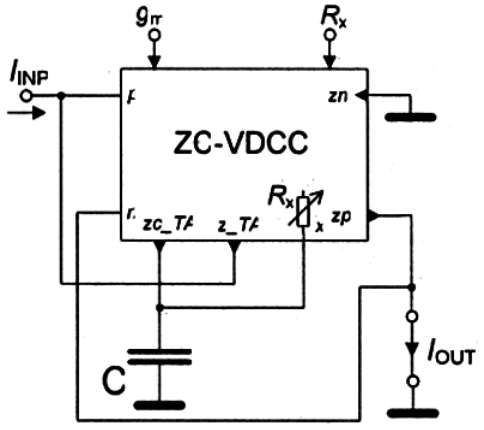

Fig. 2 — Current-mode all-pass section with independent pole and/or zero frequency control

$$K_{AP\_CM1}(s) = \frac{I_{OUT}}{I_{INP}} = \frac{g_m - sC}{g_m\left(1 + sCR_x\right)} \qquad \ldots (1)$$

where zero frequency is adjustable by g_m as $\omega_z = g_m/C$ and pole frequency $\omega_p = 1/R_xC$ can be adjusted by R_x. Disadvantage is direct influence of g_m change on *dc* gain (at low frequencies), but it can be useful for some systems, where behaviour in magnitude responses is not so important[7]. Input impedance (resistance) of this solution is proportional to $\sim 1/g_m$.

The next circuit shown in Fig. 3 is modification of previous solution, where different interconnection of terminals was used in order to obtain possibility of zero frequency control. Only one parameter (R_x) allows adjusting of zero frequency in inverting all-pass section.

Transfer function has form:

$$K_{AP\_CM2}(s) = \frac{I_{OUT}}{I_{INP}} = \frac{sC\left(1 - g_mR_x\right) - g_m}{sC + g_m} \qquad \ldots (2)$$

from which zero frequency is $\omega_z = \dfrac{g_m}{\left(1 - g_mR_x\right)C}$.

Zero is in right-half-plane (RHP) of the complex space for typical all-pass configuration ($g_mR_x > 1$). Controllable parameter R_x allows change of transfer function from all-pass section to inverting transfer section with migration of zero to left-half-plane (LHP). Input impedance of this circuit is frequency dependent and directly proportional to R_x value.

The circuit shown in Fig. 4 has advantage of independent zero and also pole frequency control. We can found transfer function in the form:

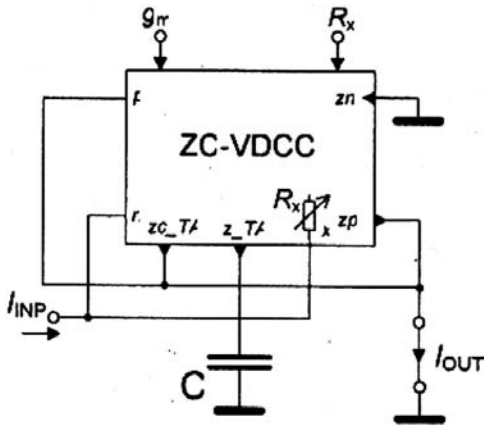

Fig. 3 — Current-mode all-pass section with independent zero frequency control

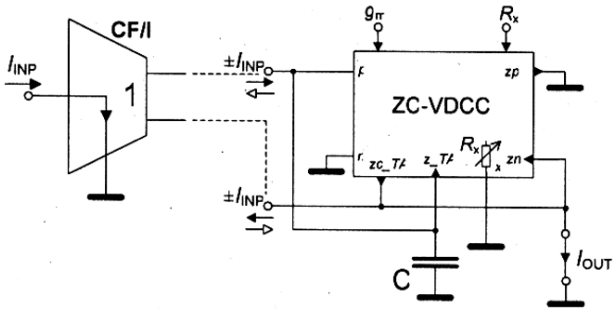

Fig. 4 — Current-mode non-inverting/inverting all-pass section with independent zero and/or pole frequency control and low-impedance input

$$K_{AP\_CM3}(s) = \frac{I_{OUT}}{I_{INP}} = \pm\frac{1 - sCR_x}{R_x(g_m + sC)} \qquad \ldots (3)$$

where $\omega_z = 1/R_xC$ and $\omega_p = g_m/C$. Hence, both adjustable parameters of the VDCC are used effectively. On the other hand, this structure requires current excitation to two nodes (input currents of both polarities). Interchange of their polarity changes overall polarity of the transfer (as included in Eq. 3). The current distributor (current follower/inverter – CF/I with two outputs) is required for this operation. Simultaneous control of R_x and g_m allows to work as typical all-pass filter. Influence of R_x on *dc* gain is the drawback of this solution. However, it is not critical problem in some cases[7]. Input impedance of this circuit is low (given by input impedance of used CF/I). Therefore, solution is immediately suitable for cascading.

Output of discussed solutions has frequency dependent high-impedance character given by parameters and values of passive elements. It is not important if next connected block has sufficiently low-impedance current input. Output node of all proposed circuits in this subsection has to be connected to the low-impedance input (shorted in ideal case) of following system for correct operation.

3.2 Mixed-Mode All-pass Section

Interesting mixed-mode solution of all-pass filter is shown in Fig. 5. The circuit behaves as voltage to current converter with all-pass characteristic. The trans-admittance-mode (TAM) transfer function has the following form:

$$K_{AP\_TAM}(s) = \frac{I_{OUT}}{V_{INP}} = g_m\left(\frac{1 - sCR_x}{1 + sCR_x}\right). \qquad \ldots (4)$$

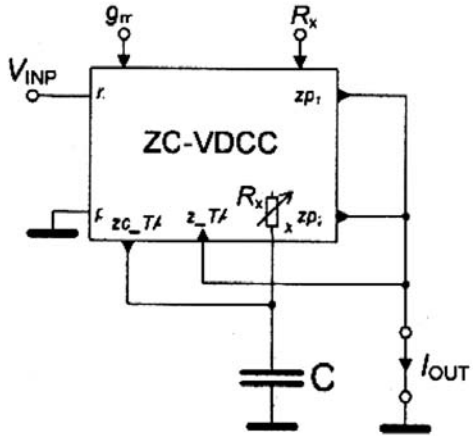

Fig. 5 — Mixed-mode all-pass section with electronic control of zero/pole frequency and also of conversion gain

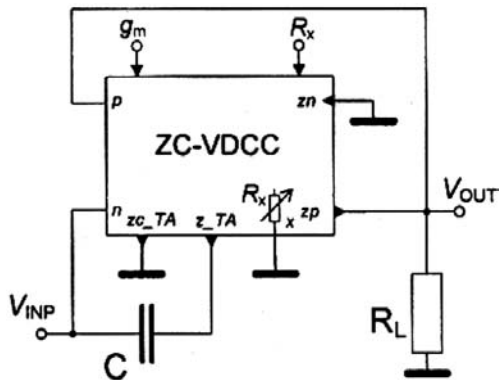

Fig. 6 — Voltage-mode all-pass section utilizing floating capacitor and grounded resistor.

Electronic control of zero/pole frequency by R_x and also independent electronic control of conversion *dc* gain by g_m are the main advantages of this circuit. Presented structure requires two positive *zp* terminals in comparison to the rest of discussed solutions in this section. Current-mode all-pass section is also possible in this structure, when grounded resistor (small value) is connected to the input terminal (V_{INP}) – this resistance realizes current to voltage conversion.

Input impedance of the solution shown in Fig. 5 is high (and frequency independent) and character of the output of the circuit is similar to current-mode solutions in section 3.1 (low-impedance input of a following block is required).

3.3 Voltage-Mode All-pass Sections

Very simple utilization of ZC-VDCC in voltage-mode all-pass sections is also possible. Circuit shown in Fig. 6 uses floating capacitor and grounded external resistor. Despite fact of floating capacitor, it allows

simultaneous control of both pole and zero frequency and therefore, simple application as adjustable phase shifter. Similar method of utilizing OTA section and inverting buffered amplifier with floating capacitor was proposed by Herencsar *et al*[30].

Transfer function was obtained as:

$$K_{AP\_VM1}(s)=\frac{V_{OUT}}{V_{INP}}=\frac{R_L\left(g_m-sC\right)}{g_mR_L+sCR_x} \qquad \ldots (5)$$

where simple simultaneous tuning of zero and pole by g_m is allowed, if we suppose matching of $R_L = R_x$. Generally, pole frequency is controllable independently by $R_x\left(\omega_p=\frac{g_mR_L}{CR_x}\right)$. Input impedance of this circuit is frequency dependent, but buffering is not required in case of excitation from standard low-impedance voltage source – output of the operational amplifier in previous sub-system for example. Similarly, buffering is necessary in case of low-impedance load at the output.

Grounded resistor (which can be considered as disadvantage of this solution) can be also easily removed as presented in solution shown in Fig. 7. Modified circuit has transfer function:

$$K_{AP\_VM2}(s)=\frac{V_{OUT}}{V_{INP}}=-\frac{R_x\left(g_m-sC\right)}{1-g_mR_x+sCR_x} \qquad \ldots (6)$$

and it behaves as inverting all-pass section if $g_mR_x = 0.5$. However, electronic controllability of this circuit is complicated due to this matching condition. Character of the input and output and their interconnection with other systems is similar to previous situation (Fig. 6).

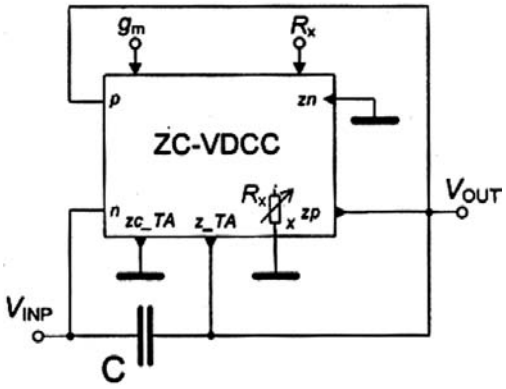

Fig. 7 — Modified voltage-mode all-pass section from Fig. 6 utilizing only floating capacitor.

Figure 8 shows better solution than circuits depicted in Figs 6 and 7. External resistor R_L is not required in this modification. Nevertheless, advantage of independent pole frequency control by R_x (Fig. 6) is missing. However, additional voltage buffer/inverter (VB/I) is necessary. Low-impedance output (practically given by output impedance of the external inverter) is substantial advantage of the solution. Transfer function is given by equation:

$$K_{AP\_VM3}(s)=\frac{V_{OUT}}{V_{INP}}=\frac{g_m-sC}{g_m+sC}. \qquad \ldots (7)$$

External voltage inverter can be omitted if current conveyor part in frame of the VDCC (Fig. 1c) has inverting transfer between Y and X terminals (so called inverting current conveyor[9]-ICCII). In such case output impedance of the all-pass section is determined by actual R_x value. Due to low-impedance output (solution with voltage inverter in Fig. 8) cascading of these blocks is easily possible.

The circuit in Fig. 9 shows the next unusual example of ZC-VDCC application and has non-typical transfer function:

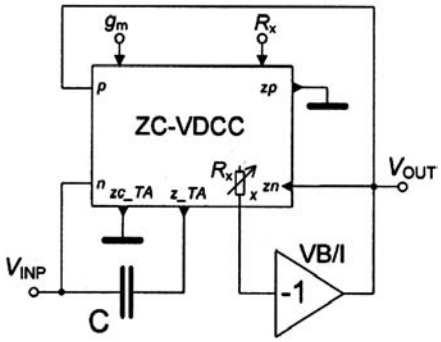

Fig. 8 — Resistor-less modification of the voltage-mode all-pass section from Fig. 6 without matching conditions.

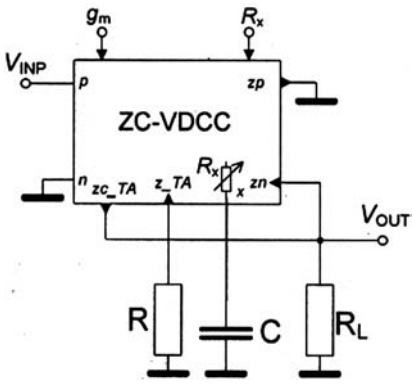

Fig. 9 — Modified voltage-mode all-pass section with independent zero frequency control.

$$K_{AP\_VM4}(s)=\frac{V_{OUT}}{V_{INP}}=g_m R_L\left[\frac{1+sC\left(R-R_x\right)}{1+sCR_x}\right] \quad \ldots(8)$$

that has interesting feature of continuous controllability of the zero location $\omega_z=\frac{1}{(R-R_x)C}$ by grounded resistance R. Similarly as in Eq.(2), it allows change the zero location from RHP to LHP. Input impedance of the circuit is frequency independent and high; therefore, cascading of such blocks is also possible. However, low-impedance load influences output significantly (voltage buffer required).

4 Experimental Verification of Selected Filter

All-pass filter from Fig. 6 was selected for experimental verification because it has advantage of simple simultaneous electronic control of zero and pole frequency. We proposed following behavioral models of VDCC based on commercially available devices employing diamond transistors[31,32] (DT) OPA660/860 and current-mode multiplier[33] (or conveyor) EL2082 in order to test selected circuit by PSpice simulations and also lab measurements.

4.1 Proposed Behavioral Models

The all-pass filter from Fig. 6 does not require all terminals (*zc_TA* and *zn*), therefore, suitable behavioral model can be simpler than proposed device as shown in Fig. 1. Two possible implementations of behavioral model of VDCC element based on DTs and EL2082 are shown in Fig. 10. Despite of fact that EL2082 is classified as obsolete element without proper replacement, this device is still available from some distributors and very useful for behavioral experiments.

These preliminary tests with both behavioral models of VDCC suppose R_x and g_m parameters controllable as external parts. Both g_m and also R_x parameter should be controllable by bias currents in practical CMOS utilization of VDCC element, but that is not the purpose of the present paper.

4.2 Measurement and Simulation Results

All-pass filter as shown from Fig. 6 was designed with following parameters: $f_p=f_z=1.59$ MHz, $C=$ 100 pF, $R=R_x=1$ kΩ, $g_m=1$ mS. Proposed application was verified with behavioral model shown in Fig. 10b by simulations and experiments with commercially available devices, oscilloscope

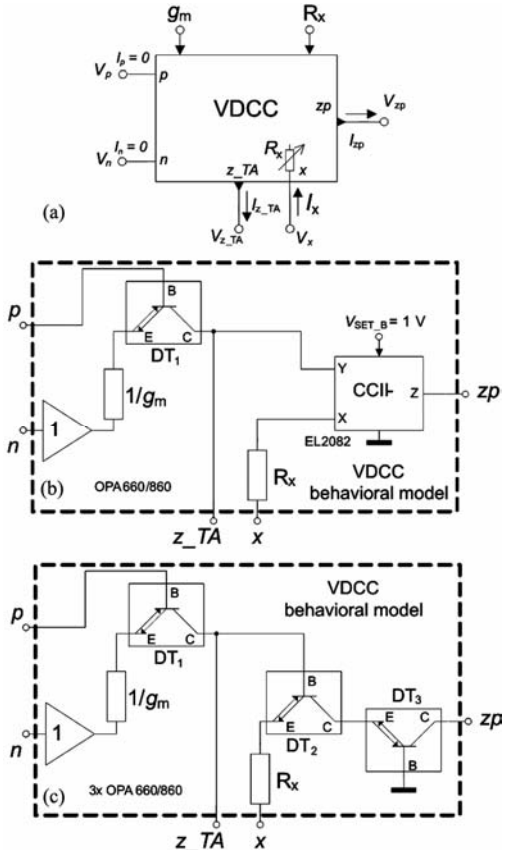

Fig. 10 — Possible implementation of reduced behavioral model of ZC-VDCC: (a) symbol, (b) using OPA 660/860 and EL2082, (c) utilizing OPA660/860 only.

DS1204B, and vector-network analyzer Agilent E5071C. Supply voltage was ± 5 V. Measured results in frequency domain (magnitude and phase characteristics in detail from 100 kHz to 100 MHz) are shown in Fig. 11. Available frequency bandwidth of the proposed prototype is about 20 MHz. Measured value of $f_p=f_z$ was 1.525 MHz. Transient response of the output signal for excitation frequency 1.5 MHz, that is very close to pole and zero frequency of the all-pass section, as shown in Fig. 12. Input signal (CH1) is plotted by blue colour and output signal by red colour (CH2). Tune ability of the section was verified by discrete changes of transconductance g_m with particular values: 0.21, 0.45, 1.0 and 2.21 mS (by resistor $1/g_m$ in Fig. 10b). Ideal $f_p=f_z$ values are 0.334, 0.716, 1.591, and 3.374 MHz, while by simulations provided values are 0.349, 0.707, 1.494, and 3.088 MHz. Results obtained from experimental tests with behavioral model are: 0.367, 0.683, 1.525, and 3.261 MHz. Simulated and measured phase characteristics of the all-pass section are compared in

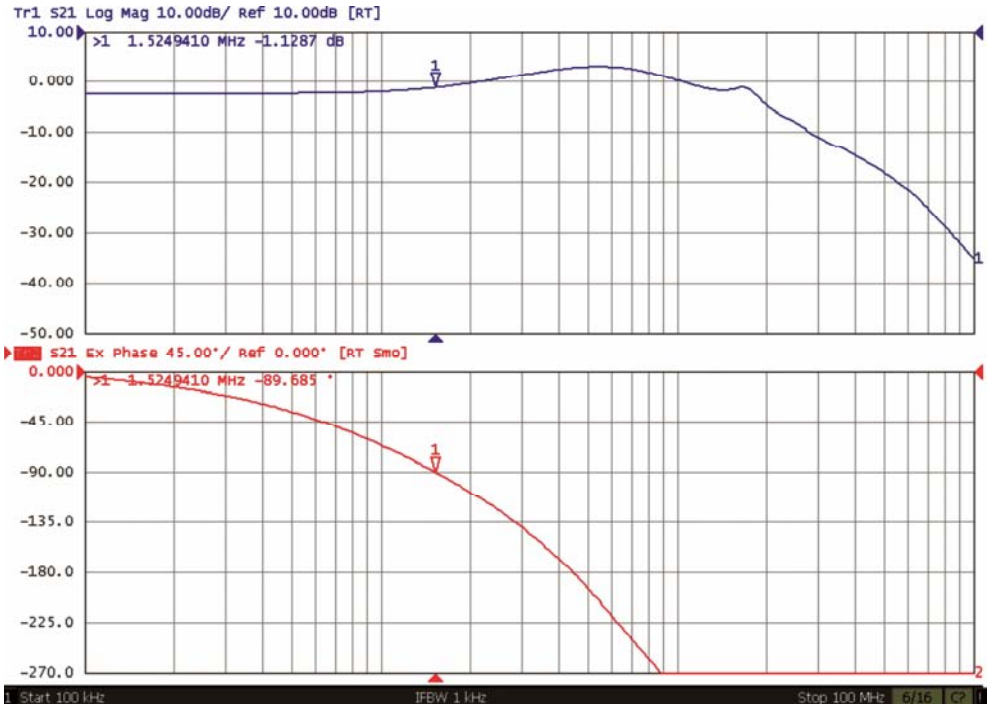

Fig. 11 — Measured results of the all-pass section – detail of magnitude and phase response

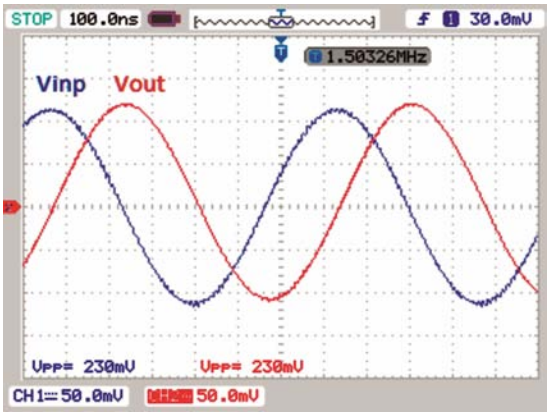

Fig. 12 — Input and output transient responses of AP filter for sine wave excitation

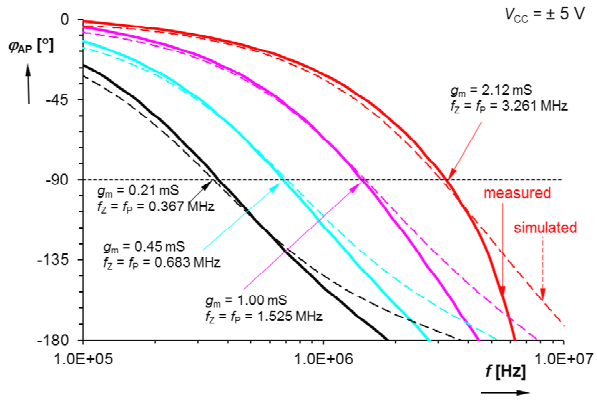

Fig. 13 — Comparison of simulated and measured phase responses for different values of g_m.

Fig. 13. All results were obtained for 50 Ω input and output matching conditions.

4.3 Analysis of Parasitic Effects

The circuit model of the all-pass section (Fig. 6) including real parasitics is shown in Fig. 14. Current and voltage error of current conveyor section in frame of ZC-VDCC are signed as α (voltage tracking error between *z_TA* and *x* terminal) and β (current tracking error between *x* and *zp* terminal). Their values are given by: $\alpha = 1 - \varepsilon$ and $\beta = 1 - \delta$, where $|\varepsilon| << 1$ and $|\delta| << 1$. Parasitic elements have values determined from interconnection of terminals of commercially available devices that were selected for experimental verification. We expect $R_{p1} \approx 25$ kΩ (output[31] of the OPA660 and input[33] Y of the EL2082 are in parallel), $C_{p1} \approx 6$ pF (4+2 pF), $R' = R_L \| R_p \| R_{zp} \approx 1$ kΩ ($R << R_p \| R_{zp}$ and has dominant impact) and $C_{p2} \approx 7$ pF (2+5 pF). Resistance R_x (95+910 Ω) is considered as parasitic in many works in the field. However, it is used often for electronic control[34]. In this case, R_x is

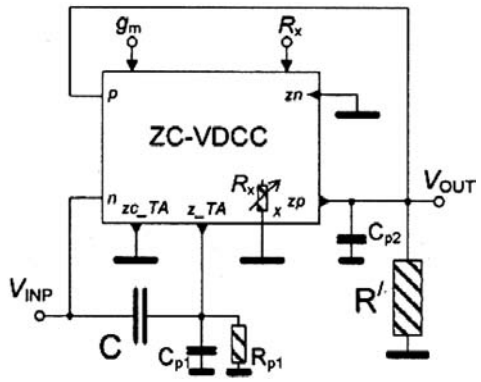

Fig. 14 — Filter from Fig. 6 including parasitics for study of parasitic influences.

correct function of the proposed circuit. Transfer function including above discussed parasitic elements and parameters have form:

$$K'_{AP\_VM1}(s) = \frac{\alpha\beta R_{p1}\left(R' g_m - sC_1R'\right)}{s^2C_{p2}\left(C_1 + C_{p1}\right)R'R_xR_{p1} + \\ + s\left(C_{p1}R_{p1} + C_1R_{p1} + C_{p2}R'\right)R_x + \\ + R_x + \alpha\beta R_{p1}R' g_m} \quad \ldots(9)$$

necessary for Eq. (9) has the denominator of the second order. The zero is still located at $f_z \cong 1.591$ MHz, but two poles exist in real case. Numerical calculation provided their values as $f_{p1} \cong 1.67$ MHz and $f_{p2} \cong 21.1$ MHz. Therefore, drop of magnitude response in direction to the high frequencies is caused mainly by the second pole. The main source of this problem is C_{p2}. The frequency where phase shift is equal to 90 degree was found as 1.518 MHz (first pole). Therefore, measurement results (Figs 11 and 13) are quite near to real behaviour expectation from this non-ideal analysis.

5 Conclusions

Several introduced simple applications of VDCC prove suitability of this active element for design of special and simple parts of communication sub-systems (in this contribution all-pass sections). The circuit in Fig. 2 allows completely independent electronic control of the zero and pole frequencies. Circuit in Fig. 3 has benefit of simple electronic control of migration of zero from RHP to the LHP. The solution in Fig. 4 also allows independent zero and pole control, but circuit requires additional current distribution to two input nodes. Figure 5 shows circuit with mixed-mode application (voltage input and current output). Zero and pole frequency are adjustable simultaneously and *dc* gain constant between input voltage and output current is controllable independently. Figure 6 offers solution, where simultaneous control of zero/pole frequency is easily possible by g_m. Separated pole frequency control is also possible in this case. External resistor could be saved, but matching condition is more complicated than in previous type of all-pass filter, see Fig. 7. Resistor-less all-pass filter was introduced also in Fig. 8. However, correct operation of such system requires additional external voltage inverter. Fortunately, the same function is available, if in internal VDCC topology the current conveyor (CCII) is changed to ICCII (but we lost advantage of low-impedance output consequently). All-pass filter in Fig. 9 provides control of zero migration by grounded resistor that allows to implement external system for its control (digital potentiometer, digital to analog converter, CMOS resistance equivalent, …) independent on features of VDCC fabricated in specific topology. One of presented solution was chosen (Fig. 6) to be verified experimentally and results confirmed expected behaviour and also tunability of all-pass filter. Proposed behavioral model of VDCC allows operation of circuit in bandwidth of units MHz with sufficient dynamics and it is suitable also for preliminary experimental tests of other applications.

Acknowledgement

Research described in this paper was financed by Czech Ministry of Education in frame of National Sustainability Program under grant LO1401. For research, infrastructure of the SIX Center was used.

References

1 Gift S J G, *Microelectronics Journal*, 31 (2000) 9.
2 Jaikla W & Promee P, *Radioengineering*, 20 (2011) 594.
3 Promee P & Somdunyakanok M, *35th Int Conf on Telecommunications and Signal Processing (TSP2012)*, Prague, (2012) 355.
4 Valsa J & Vlach J, *Int J of Circuit Theory & Applications*, 41 (2013) 59.
5 Radwan A G, Elwakil A S & Soliman A M, *IEEE Trans on Circuits & Sys,* 55 (2008) 2051.
6 Radwan A G, Elwakil A S & Soliman A M, *J of Circuits, Sys & Computers*, 17 (2008) 55.
7 Petrzela J, *23th Int Conf Radioelektronika*, Czech Republic, (2013) 182.
8 Maundy B, Elwakil A & Gift S, *Circuits Systems & Signal Proc*, 31 (2012) 3.

9 Biolek D, Senani R, Biolkova V & Kolka Z, *Radioengineering*, 17 (2008) 15.
10 Sedra A & Smith K C, *IEEE Trans on Circuit Theory*, 17 (1970) 132.
11 Fabre A, Saaid O, Wiest F & Boucheron C, *IEEE Trans on Circuits & Sys,* 43 (1996) 82.
12 Surakampontorn W & Thitimajshima W, *IEE Proceedings-G*, 135 (1988) 71.
13 Fabre A & Mimeche N, *Electronics Lett*, 30 (1994) 1267.
14 Geiger R L & Sánchez-Sinencio E, *IEEE Circ & Devices Magazine*, 1 (1985) 20.
15 Prokop R & Musil V, *Proc Conf on Signal & Image Proc IASTED*, Anaheim, (2005) 494.
16 Kumar P, Pal K & Gupta G K, *Indian J of Pure & Appl Phys*, 44 (2006) 398.
17 Sharma S, Rajput S S, Pal K, Mangotra L K & Jamuar S S, *Indian J of Pure & Appl Phys*, 44 (2006) 871.
18 Tangsrirat W, Channumsin O & Pukkalanun T, *Indian J of Pure & Appl Phys*, 51 (2013) 516.
19 Shah N A, Quadri M & Iqbal S Z, *Indian J of Pure & Appl Phys*, 46 (2013) 893.
20 Minaei S & Ibrahim M A, *Int J Electronics*, 92 (2005) 347.
21 Maheshwari S, *Circuits Sys & Signal Proc*, 27 (2008) 123.
22 Minaei S & Yuce E, *Circuits Sys & Signal Proc*, 29 (2010) 391.
23 Horng J W, *Radioengineering*, 19 (2010) 653.
24 Ibrahim M A, S Minaei & Kuntman H, *Int J of Electronics & Communi*, 59 (2005) 311.
25 Ibrahim A M, Kuntman H & Cicekoglu O, *Circuits Sys & Signal Processing*, 22 (2003) 525.
26 Metin B, Cicekoglu O & Pal K, *Midwest Symposium on Circuits & Sys*, Montreal, (2007) 518.
27 Krishna M, Kumar N, A Srinivasulu & Lal R K, *Int Conference on Circuits, Systems,* (2011) 128.
28 Chatuverdi B & Maheshwari S, *J Communication & Computer*, 9 (2012) 613.
29 Ibrahim M A, Kuntman H, *Int J Electronics & Communication*, 58 (2004) 429.
30 Herencsar N, Minaei S, Koton J, Yuce E & Vrba K, *Analog Integrated Circuits & Signal Proc*, 74 (2013) 141.
31 *Texas Instruments. OPA660 Wide bandwidth operational transconductance amplifier and buffer (datasheet)*, (2000) 20, accessible on www: http://www.ti.com/lit/ds/symlink/opa660.pdf
32 *Texas Instruments. OPA860 Wide-bandwidth, operational transconductance amplifier (OTA) and buffer (datasheet)*, (2008) 33, accessible on www: http://www.ti.com/lit/ds/symlink/opa860.pdf
33 *Intersil (Elantec). EL2082 CN Current-mode multiplier* (datasheet), (1996) 14, accessible on www: http://www.intersil.com/data/fn/fn7152.pdf
34 Sotner R, Kartci A, Jerabek J, Herencsar N, Dostal T & Vrba K, *Measurement Sci Review,* 12 (2012) 255.